British Journal of Clinical Pharmacology

Br J Clin Pharmacol (2017) **83** 1758–1772 1758

PHARMACOKINETIC DYNAMIC RELATIONSHIPS

Population pharmacokinetics and pharmacodynamics of linezolid-induced thrombocytopenia in hospitalized patients

Correspondence Dr Yasuhiro Tsuji PhD, Department of Medical Pharmaceutics, Faculty of Pharmaceutical Sciences, University of Toyama, 2630 Sugitani, Toyama, 930-0194, Japan. Tel./Fax: + 81 76 434 7584; E-mail: ytsuji@pha.u-toyama.ac.jp

Received 22 September 2016; **Revised** 9 January 2017; **Accepted** 3 February 2017

Yasuhiro Tsuji[1,2], Nicholas H.G. Holford[2], Hidefumi Kasai[1,3], Chika Ogami[1], Young-A Heo[2], Yoshitsugu Higashi[4], Akiko Mizoguchi[5], Hideto To[1] and Yoshihiro Yamamoto[4]

[1]Department of Medical Pharmaceutics, Faculty of Pharmaceutical Sciences, University of Toyama, Toyama, Japan, [2]Department of Pharmacology and Clinical Pharmacology, University of Auckland, Auckland, New Zealand, [3]Certara G.K., Tokyo, Japan, [4]Department of Clinical Infectious Diseases, Graduate School of Medicine and Pharmaceutical Sciences for Research, University of Toyama, Toyama, Japan, and [5]Department of Pharmacy, Sasebo Chuo Hospital, Nagasaki, Japan

Keywords linezolid, methicillin-resistant *Staphylococcus aureus*, mixture model, pharmacometrics, thrombocytopenia, turnover model

AIMS

Thrombocytopenia is among the most important adverse effects of linezolid treatment. Linezolid-induced thrombocytopenia incidence varies considerably but has been associated with impaired renal function. We investigated the pharmacodynamic mechanism (myelosuppression or enhanced platelet destruction) and the role of impaired renal function (RF) in the development of thrombocytopenia.

METHODS

The pharmacokinetics of linezolid were described with a two-compartment distribution model with first-order absorption and elimination. RF was calculated using the expected creatinine clearance. The decrease platelets by linezolid exposure was assumed to occur by one of two mechanisms: inhibition of the formation of platelets (PDI) or stimulation of the elimination (PDS) of platelets.

RESULTS

About 50% of elimination was found to be explained by renal clearance (normal RF). The population mean estimated plasma protein binding of linezolid was 18% [95% confidence interval (CI) 16%, 20%] and was independent of the observed concentrations. The estimated mixture model fraction of patients with a platelet count decreased due to PDI was 0.97 (95% CI 0.87, 1.00), so the fraction due to PDS was 0.03. RF had no influence on linezolid pharmacodynamics.

CONCLUSION

We have described the influence of weight, renal function, age and plasma protein binding on the pharmacokinetics of linezolid. This combined pharmacokinetic, pharmacodynamic and turnover model identified that the most common mechanism of thrombocytopenia associated with linezolid is PDI. Impaired RF increases thrombocytopenia by a pharmacokinetic mechanism. The linezolid dose should be reduced in RF.

DOI:10.1111/bcp.13262

WHAT IS ALREADY KNOWN ABOUT THIS SUBJECT

- Linezolid treatment is associated with thrombocytopenia and is more common with renal function impairment.

WHAT THIS STUDY ADDS

- Weight, renal function and age explain the variability in linezolid pharmacokinetics.
- Linezolid thrombocytopenia is most commonly due to myelosuppression rather than platelet destruction.
- Renal impairment increases linezolid exposure. Dose adjustment should reduce thrombocytopenia.

Introduction

Linezolid is a member of the oxazolidinone class of synthetic antimicrobial agents with a unique mechanism action compared with other agents in this class [1]. It has been used to treat critical infections, including pneumonia, sepsis, and wound, skin and soft tissue infections [2–6]. It has strong antibacterial activity against aerobic Gram-positive cocci (GPC), methicillin-resistant coagulase-negative staphylococci, vancomycin-resistant enterococci and methicillin-resistant *Staphylococcus aureus* (MRSA) [7, 8], and has been approved for use in more than 60 countries. MRSA represents a predominant pathogen associated with serious infections which have become a major therapeutic problem because of the associated high rates of morbidity, mortality and hospital length of stay [9, 10]. Recent prospective randomized, double-blind trials have compared the use of linezolid compared with vancomycin for the treatment of adult patients with hospital-acquired or healthcare-associated MRSA pneumonia [11], Gram-positive nosocomial pneumonia [12, 13] and Gram-positive ventilator-associated pneumonia [14]. For the treatment of these infections, the clinical response was significantly greater with linezolid than vancomycin. However, three meta-analyses comparing linezolid with glycopeptides (including vancomycin) for the treatment of nosocomial MRSA pneumonia all showed similar clinical cure and survival rates for linezolid and vancomycin [15–17]. Thus, linezolid is now considered to be one of the most important for the treatment of GPC and MRSA infections.

Linezolid is predominantly metabolized through oxidation of its morpholine ring to an inactive form by non-enzymatic oxidative reactions [1]. Dose adjustment is considered unnecessary for patients at any stage of renal dysfunction, including haemodialysis, even though clearance (CL) was found to increase by 50% during haemodialysis [18]. However, linezolid concentrations are significantly higher in patients with a renal function (RF) impairment than in those without [19–25]. In general, linezolid is administered at a dose of 600 mg twice daily orally and/or via intravenous infusion. After the initiation of linezolid treatment, the linezolid trough concentration is assumed to be maintained between 2 μg ml^{-1} and 7 μg ml^{-1} [22]. Nukui *et al.* [26] demonstrated that thrombocytopenia developed more frequently in patients with a linezolid trough concentration of >7.5 μg ml^{-1}. It has been recommended that the dose of linezolid should be adjusted based on serum concentrations [6, 27].

Thrombocytopenia and anaemia are among the most important adverse effects of linezolid treatment. The incidence of linezolid-induced thrombocytopenia and anaemia varies considerably. Thrombocytopenia has been observed in 7.4% [28] and 11.8% [29] of linezolid-treated patients, and anaemia in 4.1% [28] and 38.1% [29] of the same groups. The probability of linezolid-induced thrombocytopenia and anaemia occurring is raised after long-term administration of this drug [30]. Niwa *et al.* [31] reported that the incidence of linezolid-induced thrombocytopenia was 17% and that the use of a high dose (≥22 mg kg^{-1}) was a risk factor for this condition. In the previous studies, thrombocytopenia was observed in 32% of patients who received linezolid for more than 10 days [32], and 32.8% of those who received this treatment for more than 14 days [33]. In addition, some groups described linezolid-induced thrombocytopenia and anaemia in patients with an RF impairment [19, 21, 25, 34] and persistently high serum linezolid concentrations [23, 35].

The mechanism responsible for linezolid-induced thrombocytopenia have not been clearly elucidated. Green *et al.* [36], reported reversible myelosuppression similar to that seen with chloramphenicol. Bone marrow findings in one patient included abundant megakaryocytes, and erythroid aplasia [36]. Two studies have reported the use of linezolid exposure to predict thrombocytopenia using a turnover model assuming decreased platelet formation [34, 37]. The turnover model was based on a myelosuppression model formulated by Friberg *et al.* [38] for chemotherapy-induced neutropenia. Using a cell proliferation model, Sasaki *et al.* [34] reported that the predicted probability of thrombocytopenia during 14 days of treatment (1200 mg day^{-1}) in patients with a creatinine CL (CLcr) of 10–30 ml min^{-1} was 32.6–51.0%. Using the stem cell model, Boak *et al.* [37] reported that a linezolid concentration of 8 μg ml^{-1} inhibited the synthesis of platelet precursor cells by 50%. Two studies noted that the platelet count reached a nadir at 15–20 days postlinezolid treatment [34, 37]. A mechanism involving a change in platelet formation would be slow because platelet lifespan is around 8–10 days [39].

By contrast, several case reports have proposed a mechanism involving an increase in the elimination of platelets via drug-induced immune-mediated destruction [40–42]. This suggested mechanism is based on observations of an increase in megakaryocytes in bone marrow or drug-related antiplatelet antibodies, with a rapid onset of platelet decline around 3–7 days following the initiation of linezolid therapy [40, 42].

In light of this controversy about the mechanism of linezolid-induced thrombocytopenia, in the present study we investigated the possibility that either myelosuppression or enhanced platelet destruction may be important in an individual patient.

Patients and methods

Ethics

The study was performed in conformity with the Helsinki Declaration, after approval by the Ethical Review Board of University of Toyama (approval number: clinical 24–118) and Sasebo Chuo Hospital (approval number: 2012–15). Patient privacy and personal information were respected.

Patients and data sources

A summary of the data for these patients is presented in Table 1. All patients received linezolid film-coated tablets and/or injections (Zyvox®, Pfizer Inc. Tokyo, Japan) for the treatment of GPC or MRSA infections from November 2008 to August 2015 at Sasebo Chuo Hospital, Nagasaki and Toyama University Hospital, Toyama, Japan. The usual dose of linezolid was 10 mg kg^{-1} three times daily (paediatric) or 300 mg once daily to 600 mg twice daily (adult) orally and/or by intravenous drip infusion for 1–2 h. Other dosage adjustments were performed according to physicians' decisions.

Determination of linezolid concentrations

The bulk powder of linezolid for the high-performance liquid chromatography (HPLC) was provided by Pfizer Inc. All other reagents were of analytical grade and were commercially available. The serum and plasma samples were stored at −80°C until analysis. Serum and plasma deproteinized with an equivalent volume of acetonitrile, and the supernatant after centrifugation was measured by HPLC using the absolute calibration method. The unbound linezolid was obtained by

Table 1

Demographic and clinical data for the study population of patients receiving linezolid

			Observation interval	
	Number	Median	Lower 2.5%	Upper 97.5%
Total patients	81			
Male	51			
Female	30			
Administration route				
i.v	54			
p.o.	13			
Both	14			
Observed total concentration (mg l^{-1})	493	11.2	2.0	50.7
Observed unbound concentration (mg l^{-1})	380	1.9	0.3	8.8
Protein binding ratio (%)		17.0	7.6	33.3
Observed platelet count (×10^3 μl^{-1})	575	160	22	463
Observed haemoglobin level (g d l^{-1})	595	8.6	6.1	15.0
Age (years)		69	8	85
Total body weight (kg)		53.2	21.0	99.5
Infections diagnosed				
Sepsis	26			
Wound, skin and soft tissue	25			
Pneumonia	14			
Abscess	8			
Osteomyelitis	6			
Undetermined	2			
AST(IU l^{-1})		22	10	163
ALT (IU l^{-1})		20	4	190
Serum creatinine (mg dl^{-1})		0.80	0.20	7.49
CLcr (ml min^{-1})		59.6	5.6	188.4

ALT, alanine aminotransferase; AST, aspartate aminotransferase; CLcr, creatinine clearance; i.v., intravenously; PI, percentile interval; p.o., orally

centrifugation of 250 μl of the serum or plasma specimens using a Centrifree ® Ultrafiltration device (Merck Millipore Ltd, Cork, Ireland) for 30 min at 2000 *g*. Total and unbound linezolid concentrations in the serum or plasma were determined by an HPLC method using ultraviolet (UV) detection. The HPLC system (Shimadzu Corporation, Kyoto, Japan) consisted of an LC-2010 pump, an LC-2010 autosampler, an LC-2010 UV detector and an LC-2010 column oven. Data were collected and analysed using a liquid chromatography solution. Separation was carried out on an octadecyl silane Hypersil column (Cadenza 5CD-C18, 150 mm × 4.6 mm, 5 μm; Imtakt Co., Kyoto, Japan). As the mobile phase, a solution of 1% orthophosphoric acid, 30% methanol and 2 g l^{-1} heptane sulfonic acid (1:30:69) was used and the pH was adjusted to 5 by the addition of 10 M sodium hydroxide. The pump flow rate was 1.0 ml min^{-1}. The column temperature was maintained at 40°C. The wavelength of optimum UV detection was set at 254 nm. Calibration curves were linear over a concentration range of 0.1–50 μg ml^{-1} for total and unbound linezolid. The intra-/interday coefficient of variation (CV) was below 5.0%, and the lower limit of quantification ((LLOQ) was 0.1 μg ml^{-1} for both total and unbound concentrations of linezolid.

Population pharmacokinetics and pharmacodynamics (PKPD) of linezolid

Population pharmacokinetics and pharmacodynamics analysis performed the population PK parameters and data (PPP & D) method [43, 44], using the first-order conditional estimation method with interaction (FOCE-I) in the nonlinear mixed-effect modeling software NONMEM® version 7.3.0 (ICON Development Solutions, Maryland, USA). The entire procedure, including executing model runs, bootstrapping, visual predictive check (VPC) and results management, was performed in Wings for NONMEM, and graphical analysis was performed by R (version 2.8.0).

Population pharmacokinetics

The pharmacokinetic model we used assumed a two-compartment distribution model for linezolid, with first-order absorption and elimination (ADVAN13, TOL = 9). Pharmacokinetic parameters were CL, volume of the central and peripheral compartments (VC and VP, respectively), intercompartment CL (Q), absorption half-life (T_{abs}) and absolute bioavailability (F). The absorption rate constant (Ka) was calculated by dividing the natural logarithm of 2 by T_{abs}.

The between-subject variability in pharmacokinetic parameters was modelled using log-normal distribution, as shown in Equation (1). P_i is the pharmacokinetic parameter for i^{th} individual, P_{POP} is the population mean value of the parameters, and η_i is a normally distributed random variable with mean zero and variance ω^2.

$$P_i = P_{POP} \times e^{\eta_i} \quad (1)$$

The residual unidentified variability was modelled with combined proportional and additive errors of total and unbound protein concentrations, as shown in Equation (2). Y_{ij} is the j^{th} measured concentration in the i^{th} subject, Y_{PREDij} is the predicted concentration based on the model. ε_{CV} and ε_{SD} are the combined proportional and additive error model components, respectively, with mean zero and variance σ^2 for concentration. The fraction of unbound plasma protein binding was estimated from the relationship between total concentrations and unbound concentrations.

$$Y_{ij} = Y_{PREDij} \times (1 + \varepsilon_{CV}) + \varepsilon_{SD} \quad (2)$$

The fraction unbound (FU) was estimated by predicting total plasma concentration from predicted unbound concentrations in the plasma. In the five samples in which the linezolid concentrations were below the LLOQ, the value was treated as missing.

Covariate model

The factor for size (F_{SIZE}) was applied to standardize the pharmacokinetic parameters, with an assumption of a standard total body weight (TBW) of 70 kg (Equation (3)) [45, 46]. The allometric exponent (PWR) of F_{SIZE} was fixed to 0.75 for CL and Q, and 1 for VC and VP.

$$F_{SIZE} = \left(\frac{TBW}{70}\right)^{PWR} \quad (3)$$

Differences associated with age were described on the basis of the fractional change in a pharmacokinetic parameter. The factor for size (F_{AGE}) of CL (F_{AGECL}) was defined (Equation (4)) and centred around the patient's median age (in years). K_{AGECL} was the age parameter for CL. F_{AGE} of Q, VC and VP were fixed to 1.

$$F_{AGECL} = e^{(K_{AGECL} \times (AGE - AGE_{median}))} \quad (4)$$

CLcr was calculated using the Cockcroft–Gault formula [47] standardized to a TBW of 70 kg. RF was normalized to a standard CLcr ($CLcr_{STD}$) of 6 l h^{-1} 70 kg^{-1} (100 ml min^{-1} 70 kg^{-1}), as shown in Equation (5) [48, 49].

$$RF = \frac{CLcr}{CLcr_{STD}} \quad (5)$$

In the four youngest hospitalized patients (aged 1, 5, 8 and 13 years), RF was assumed to be 0.5. RF was included in the model, using a linear independent combination of renal and non-renal CL parameters, as shown in Equation (6). $CL_{OVERALL}$ is the overall population value of parameter for CL. $CL_{non\text{-}renal}$ is nonrenal CL and CL_{renal} is renal CL.

$$CL_{OVERALL} = (CL_{non-renal} \times F_{AGECL} + CL_{renal} \times RF) \quad (6)$$

The covariate factors were combined to predict linezolid CL (CL_{GRP}). Group CL includes the covariates used to

characterize that specific group's pharmacokinetic parameters (Equation (7)).

$$CL_{GRP} = CL_{OVERALL} \times F_{SIZE} \quad (7)$$

Pharmacokinetic parameter estimates are for the disposition of unbound linezolid.

Mixture model

The decrease in the number of platelets due to linezolid exposure was assumed to occur as a result of one of two mechanisms in each patient – inhibition of the formation of platelets (PDI) or stimulation of the elimination of platelets (PDS) (Figure 1).

A mixture model was used to identify the fraction (F) of patients in the study population who were best described by an inhibitory and stimulating effect of linezolid on platelet formation (Equation (8)).

$$\begin{aligned} &\text{Inhibit synthesis of platelets; } F_{POP\_inhibit} \ (0 \le F_{POP\_inhibit} \le 1) \\ &\text{Stimulate the elimination of platelets; } F_{POP\_stimulate} = 1 - F_{POP\_inhibit} \end{aligned} \quad (8)$$

Population PKPD modelling

The time course of the linezolid-induced reduction in the platelet count is based on a semi-mechanistic model for myelosuppression [38]. The model is composed of a compartment representing progenitor cells in the bone marrow, a compartment of systemic circulating platelets, and a link between them through three transit compartments reflecting platelet maturation (Equation (9)). The intercompartment transit rate constant (Ktr) was estimated from the mean transit time (MTT), so that Ktr = (1 + Ntr)/MTT, where Ntr is the number of transit compartments. Circulating platelets (PLTCIRC) were eliminated by a first-order process. The half-life of platelets (PLTHALF) was estimated and the corresponding rate constant Kcirc was calculated from the natural logarithm of 2 divided by PLTHALF. The initial platelet count in the PLTFORM, Transit 1, Transit 2 and Transit 3 compartments was calculated from PLTCIRC0 × Kcirc/Ktr and in the PLTCIRC compartment it was set to PLTZERO, where PLTZERO is the platelet count in the blood before starting linezolid.

$$\begin{aligned} \frac{d\text{PLTFORM}}{dt} &= RFORM \times \text{FBACK} \times \text{PDI} - \text{Ktr} \times \text{PLTFORM} \\ \frac{d\text{Transit 1}}{dt} &= K_{tr} \times \text{PLTFORM} - K_{tr} \times \text{Transit 1} \\ \frac{d\text{Transit 2}}{dt} &= \text{Ktr} \times \text{Transit 1} - \text{Ktr} \times \text{Transit 2} \\ \frac{d\text{Transit 3}}{dt} &= \text{Ktr} \times \text{Transit 2} - \text{Ktr} \times \text{Transit 3} \\ \frac{d\text{PLTCIRC}}{dt} &= \text{Ktr} \times \text{Transit 3} - \text{Kcirc} \times \text{PLTCIRC} \times \text{PDS} \end{aligned} \quad (9)$$

The rate of formation of platelets (RFORM) was assumed to be driven either by proliferation of cells in the platelet formation compartment (PLTFORM) or from the baseline platelet count (PLTZERO) as a constant stem cell precursor (Equation (10)).

$$\begin{aligned} &\text{RFORM} = \text{Ktr} \times \text{PLTFORM; proliferation} \\ &\text{RFORM} = \text{Ktr} \times \text{PLTZERO; stem cell} \end{aligned} \quad (10)$$

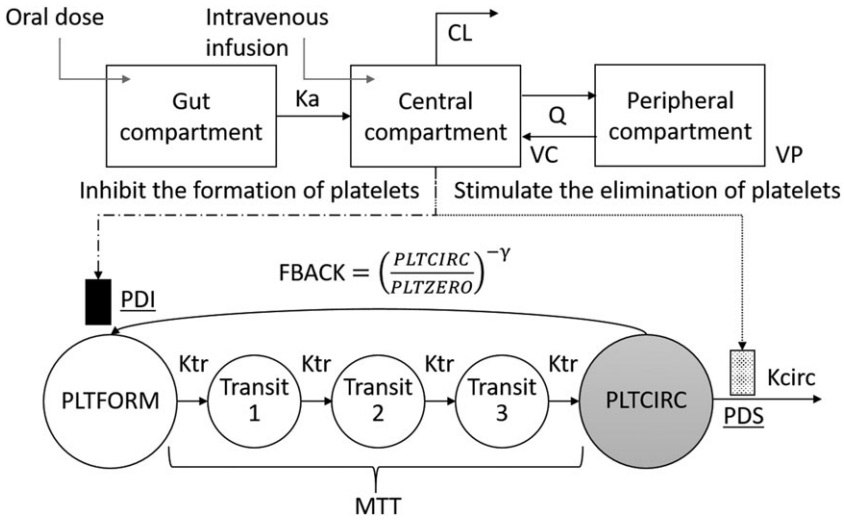

Figure 1

Schematic representation of the structural pharmacokinetic model for linezolid and pharmacodynamic model for platelet time course. CL, clearance; FBACK, empirical feedback model; Ka, absorption rate constant; Kcirc, rate constant of PLTCIRC; Ktr, intercompartment transit rate constant; MTT, mean transit time; PDI, inhibition effect; PDS, stimulation effect; PLTCIRC, circulating platelets; PLTFORM, initial rate of formation of platelets; PLTZERO, baseline platelet count; Q, intercompartment clearance; VC, volume of the central compartment; VP, volume of the peripheral compartment. The final model uses Ktr = Kcirc

An empirical feedback model (FBACK) was used to describe the effect of endogenous growth factors which change the formation rate when the platelet count changes relative to PLTZERO (Equation (11)).

$$\text{FBACK} = \left(\frac{\text{PLTCIRC}}{\text{PLTZERO}}\right)^{-\gamma} \quad (11)$$

The mechanism of action of linezolid was either through PDI on RFORM or PDS on Kcirc (Equation (12)).

$$\begin{aligned}\text{PDI} &= 1-\text{Edrug; Inhibition}\\ \text{PDS} &= 1+\text{Edrug; Stimulation}\end{aligned} \quad (12)$$

The pharmacodynamic model for linezolid (Edrug) was either a linear or an Emax model. The term Emax and C50 are the pharmacodynamic parameters defining the efficacy and potency of the drug (Equation (13)).

$$\begin{aligned}\text{Edrug} &= \text{SLOPE}\times C_{TOTAL}\text{; linear}\\ \text{Edrug} &= \frac{\text{Emax}\times C_{TOTAL}}{\text{C50}+C_{TOTAL}}\text{; Emax}\end{aligned} \quad (13)$$

The model was implemented as a system of differential equations. All compartments were initialized to PLTZERO.

Model evaluation and validation

To test the significance of various factors that influenced the PKPD parameters, the value of the objective function (OFV) determined in the NONMEM® fitting routine was used. The difference in OFV (ΔOFV) obtained by comparing each model was asymptotically distributed according to the chi-squared test, with the number of degrees of freedom (df) being equal to the difference in the number of parameters between the two models. The significance level was set at $P < 0.05$ (ΔOFV: 3.84).

A nonparametric bootstrap was used to estimate uncertainty [50]. The final model was fit repeatedly to 100 additional bootstrap datasets. The average, standard deviation (SD), relative standard error (%RSE) and 95% confidence intervals (CIs) were calculated from the empirical bootstrap distribution and compared estimates from the original dataset. A prediction-corrected VPC (pcVPC) was used to check the distribution of observed and predicted percentiles [51]. The VPC was evaluated by comparing the observed concentrations with 90% percentile intervals (PIs) and 95% CIs simulated from the final parameters.

Results

Population pharmacokinetics of linezolid

A total of 493 blood total linezolid concentrations and 380 unbound linezolid concentrations from 81 patients were available for developing the population pharmacokinetic model. There was no improvement in the fit (ΔOFV −3.73, df = 2, $P = 0.15$) compared with a previously described model [52] involving a time-related effect of linezolid exposure to reduce elimination CL. The final model contained nine estimated pharmacokinetic parameters.

Plasma protein binding was linearly related to the unbound linezolid concentration. There was no improvement in the fit when a saturable binding model was used (ΔOFV −0.522, df = 2, $P = 0.77$). The population-estimated protein binding percentage was 18%. There was no detectable population parameter variability for the unbound fraction. The pharmacokinetic parameter estimates from the original data and the bootstrap distribution are presented in Table 2.

The pharmacokinetic model parameters are shown in Equation (14).

$$\begin{aligned}\text{CL (L/h)} &= \left(1.86\times e^{-0.0205\times(\text{AGE}-69)}+1.44\times\text{RF}\right)\times\left(\frac{\text{TBW}}{70}\right)^{0.75}\text{VC (L)}\\ &= 22.9\times\left(\frac{\text{TBW}}{70}\right)\text{VP (L)} = 24.7\times\left(\frac{\text{TBW}}{70}\right)\text{Q (L/h)}\\ &= 10.9\times\left(\frac{\text{TBW}}{70}\right)^{0.75}\end{aligned} \quad (14)$$

The pharmacokinetic model described the observed data well. The model validation using pcVPC also confirmed an acceptable agreement between the observed data and model-based simulated values (Figure 2 and Figure 3). The median of the observed values was within the 95% CI of the predictions but tended to be higher than the median prediction.

Mixture model

A total of 575 platelet counts, from 80 patients, were available for developing the turnover and pharmacodynamic model. The estimated mixture model fraction of patients with a platelet count that was decreased owing to PDI was 0.97 ($F_{POPinhib}$); therefore, the fraction due to PDS ($F_{POPstim}$) was 0.03 Based on the assignment of patients to each mechanism, 78 patients had platelet formation inhibited, and two patients platelet loss stimulated with linezolid treatment.

Population PKPD modelling

A model with three transit compartments adequately described the time course of thrombocytopenia. A more complex model with 30 compartments for platelet formation and elimination [37] did not improve the fit.

A linear pharmacodynamic model was chosen to describe PDI, and an Emax model for PDS. RF was investigated to see if it affected the linezolid slope in PDI model. RF had no significant effect on the slope (ΔOFV −0.704, df = 1, $P = 0.4$). Modelling platelet turnover using the proliferation of cells in the formation compartment significantly improved the fit when compared with a stem cell precursor (ΔOFV −80.772, df = 0). The fit was not worsened by assuming that Kcirc was the same as Ktr, so we assumed that Kcirc = Ktr. Removing the feedback component of the model worsened the fit considerably (ΔOFV 169.8, df = 1, $P < 0.01$).

The final model contained eight estimated parameters, including a mixture parameter. The results of the pharmacodynamic parameter estimates of the final model, and

Table 2

Comparison of population pharmacokinetic–pharmacodynamic parameter estimates for the final model with estimates from 100 bootstrap samples

Parameter	Description	Units	Final model estimate	Bootstrap sample estimates			
				Average	95% PI		RSE%
					Lower 2.5%	Upper 97.5%	
Population mean							
Pharmacokinetics							
$CL_{nonrenal}$	Nonrenal clearance	l h^{-1}	1.86	1.76	1.29	2.17	14%
CL_{renal}	Renal clearance	l h^{-1}	1.44	1.42	0.83	2.20	25%
VC	Volume of the central compartment	l	22.9	19.3	8.1	29.4	29%
VP	Volume of the peripheral compartment	l	24.7	24.4	16.7	34.2	18%
Q	Intercompartment clearance	l h^{-1}	10.9	10.5	2.3	23.5	90%
T_{abs}	Absorption half-life	h	3.61	5.07	2.13	19.26	70%
F	Absolute bioavailability		0.922	0.895	0.747	0.999	8%
K_{AGECL}	Age parameter for CL		–0.021	–0.021	–0.030	–0.009	–25%
FU	Fraction of unbound protein binding		0.823	0.823	0.809	0.836	1%
Pharmacodynamics							
$F_{Inhibit}$	Fraction of patients with inhibition of platelet synthesis		0.969	0.949	0.867	1	3%
MTT	Mean transit time	h	113.0	103.5	65.4	130.0	15%
γ	Feedback parameter		–0.187	–0.164	–0.258	–0.061	–29%
PLTZERO	Baseline platelet count	μl^{-1}	206 000	204 451	174 000	234 100	8%
SLOPE	Slope of inhibition effect (total plasma concentration)	1/(mg l^{-1})	0.00566	0.00507	0.00248	0.00725	23%
SMAX	Maximal extent of stimulation effect		2.55	2.31	0.03	4.06	43%
SC50	Linezolid total plasma concentration producing 50% of the maximum stimulation effect	mg l^{-1}	0.00364	0.324	0.00004	1.405	339%
Between-subject variability (BSV[a])							
CL			0.369	0.366	0.267	0.464	14%
VC			1.421	1.518	1.065	2.348	22%
VP			0.050	0.206	0.024	0.629	78%
Q			1.822	1.624	0.585	2.447	31%
T_{abs}			0 FIXED				
F			0 FIXED				
MTT			0.239	0.205	0.002	0.444	66%
γ			0.307	0.225	0.003	0.521	82%
PLTZERO			0.570	0.567	0.437	0.669	10%
SLOPE			0.473	0.482	0.176	0.759	33%
SMAX			0 FIXED				
SC50			0 FIXED				
Residual unidentified variability (RUV[b])							
RUV_{PROP_TOTAL}	Proportional residual unidentified variability of total concentration		0.318	0.311	0.258	0.356	7%

(*continues*)

Table 2

(Continued)

Parameter	Description	Units	Final model estimate	Bootstrap sample estimates			
				Average	95% PI		RSE%
					Lower 2.5%	Upper 97.5%	
RUV_{ADD_TOTAL}	Additive residual unidentified variability of total concentration	mg l^{-1}	0.251	0.301	0.003	0.806	77%
$RUV_{PROP\_UNBOUND}$	Proportional residual unidentified variability of unbound protein concentration		0.319	0.313	0.256	0.357	8%
$RUV_{ADD\_UNBOUND}$	Additive residual unidentified variability of unbound protein concentration	mg l^{-1}	0.034	0.061	0.000	0.729	284%
RUV_{PROP_PLT}	Proportional residual unidentified variability of unbound protein concentration		0.234	0.242	0.204	0.273	8%

PI, percentile interval; RSE%, relative standard error
[a]BSV calculated from Square root (sqrt) (NONMEM OMEGA) [b]RUV estimated using THETA

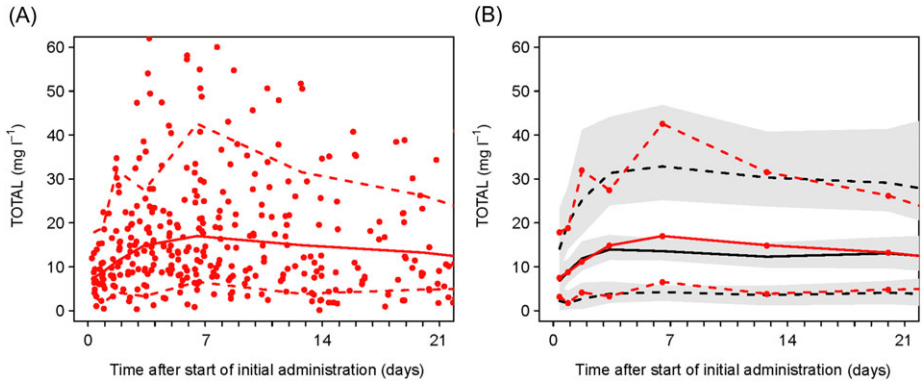

Figure 2

Model qualification using prediction-corrected visual predictive checks (pcVPC) for total linezolid concentration. (A) Prediction-corrected scatterplot of the measurements with 5th, 50th and 95th percentiles. (B) pcVPC showing the 5th, 50th and 95th percentiles for observed and predicted values. Black dashed lines, 5th to 95th percentiles of the predicted linezolid concentrations; black solid line, median predicted linezolid concentration in 100 simulated subsets of total dataset; grey-shaded areas, 95% confidence intervals of the prediction percentiles; red dashed lines, 5th and 95th percentiles of the observed linezolid concentrations; red circles, observed linezolid concentration; red solid line, median observed concentration; TOTAL, total linezolid concentration

bootstrap parameter average and 95% empirical bootstrap percentiles from 100 bootstraps are presented in Table 2. The %RSEs were small (<30%) for most PKPD and turnover parameters. Even though the fit was better with an Emax model than a linear model (ΔOFV: 21.080, df = 2, $P = 0.01$), the bootstrap %RSE of the maximal extent of the stimulation effect (SMAX) and linezolid total plasma concentration producing 50% of the maximum stimulation effect (SC50) were large (43% and 339%, respectively), indicating that the SC50 estimate was particularly uncertain. The model evaluation using pcVPC confirmed an acceptable agreement between the observed data and model-based simulated values (Figure 4). The median of the observed values was within the 95% CI of the predictions.

A simulation model was used to demonstrate linezolid-induced thrombocytopenia in patients using parameter estimates from the combined PKPD and turnover model. Simulations of predicted platelet count for the PDI and PDS models were performed with linezolid 600 mg every 12 h for at least 2 weeks, as shown in Figure 5.

When PDI was assumed, the predicted nadir of the platelet count occurred at 14 days after linezolid administration. By contrast, when PDS was assumed, the platelet count dropped sharply, to reach the predicted nadir after 2 days.

The platelet count and linezolid concentration profiles for representative patients with different dosage and linezolid administration periods are also shown in Figure 6. Three representative patients with PDI (ID 1, 58 and 64) and the two

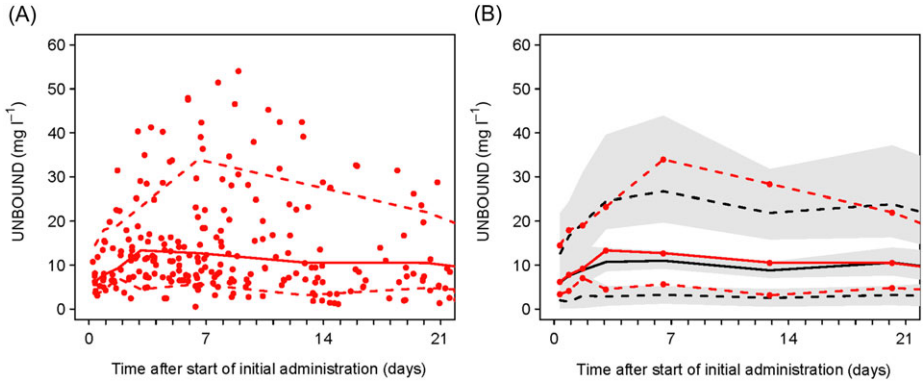

Figure 3

Model qualification using prediction-corrected visual predictive checks (pcVPC) for the unbound plasma linezolid concentration. (A) Prediction-corrected scatterplot of the measurements with 5th, 50th and 95th percentiles. (B) pcVPC showing the 5th, 50th and 95th percentiles for observed and predicted values. Black dashed lines, 5th to 95th percentiles of the predicted linezolid concentrations; black solid line, median predicted linezolid concentration in 100 simulated subsets of total dataset; grey-shaded areas, 95% confidence intervals of the prediction percentiles; red circles, observed linezolid concentration; red dashed lines, 5th and 95th percentiles of the observed linezolid concentrations; red solid line, median observed concentration; UNBOUND, unbound linezolid concentration

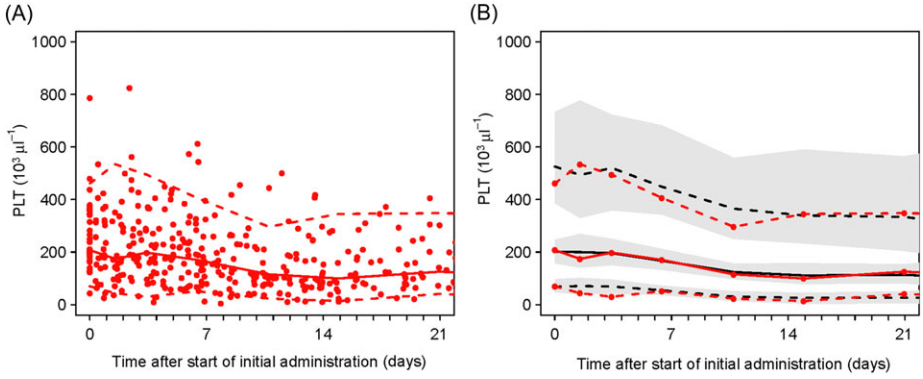

Figure 4

Model qualification using prediction-corrected visual predictive checks (pc-VPC) for platelet counts (mixture group 1 – inhibition of proliferation). (A) Prediction-corrected scatterplot of the measurements with 5th, 50th and 95th percentiles. (B) pcVPC showing the 5th, 50th and 95th percentiles for observed and predicted values. PLT, platelet count (mixture group 1). Grey-shaded areas, 95% confidence intervals of the prediction percentiles; red circles, observed platelet counts; red dashed lines, 5th and 95th percentiles the observed platelets count; red solid line, median observed platelet count; black dashed lines, 5th to 95th percentiles of the predicted platelets count; black solid line, median predicted platelet count in 100 simulated subsets of total dataset

patients with PDS (ID 37 and 55) are shown. The profiles of individual predicted values and observed values for both the PDI and PDS models were close to each other.

Discussion

Prior to the present study, the mechanism of linezolid-induced thrombocytopenia had not yet been elucidated. In the current study, we tried to identify patterns of platelet count associated with two fundamental types of mechanism for thrombocytopenia. A population PKPD modelling approach was applied to predict linezolid-associated effects on platelet turnover due either to myelosuppression or enhanced platelet destruction after oral and/or intravenous infusion of linezolid administered to patients with MRSA infections. By identifying different time courses of thrombocytopenia, we hoped to help clinicians to recognize linezolid-induced thrombocytopenia and understand how to manage linezolid dosing in patients with MRSA.

The population pharmacokinetics of linezolid have been previously described using noncompartmental and compartmental models [20, 24, 34, 37, 52–60]. The pharmacokinetic analysis in the present study was performed using a two-compartment model with first-order absorption and first-order elimination.

Both the unbound and total plasma concentrations of linezolid were modelled simultaneously. It is generally accepted that only unbound concentrations are responsible

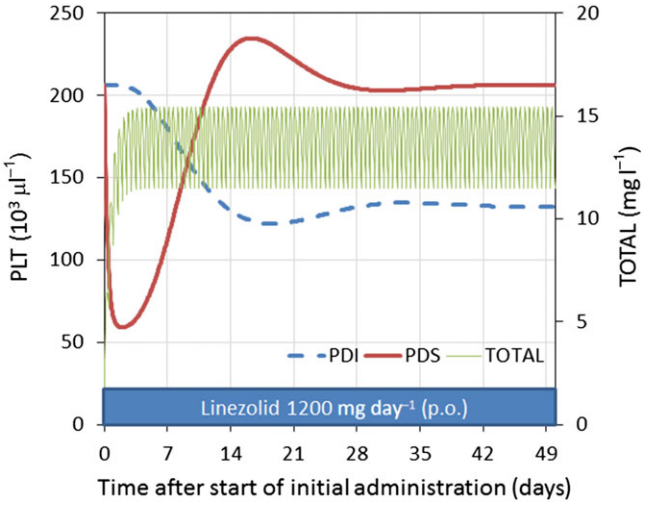

Figure 5

Predicted time course of total linezolid plasma concentration and platelet count with inhibition of proliferation (PDI) or stimulation of destruction (PDS) produced by linezolid 1200 mg day^{-1} orally. Simulation using mean values for parameters based on the final model (total body weight 70 kg, creatinine clearance 6 l h^{-1} 70 kg^{-1}, age 69 years, linezolid oral dosage 600 mg every 12 h). TOTAL, total linezolid concentration

for pharmacologically beneficial activity and side effects [61–65]. Most previous reports have been limited to the use of total concentrations [20, 24, 34, 37, 52–60]. The estimated protein binding of linezolid in the blood was 18%. There was no detectable between-subject variability in FU or the variation in FU with the observed concentrations. This result is in agreement with previous studies on linezolid pharmacokinetics [66–68].

We used TBW and theory-based allometry to identify the relationship between body size and pharmacokinetic parameters. Brier *et al.* [18] reported that the CL of linezolid did not change with RF. Other studies have not investigated whether RF influences the CL of linezolid [52–60].

Taubert *et al.* [60] described that fibrinogen and antithrombin concentrations, lower concentrations of lactate and the presence of acute respiratory distress syndrome were significant covariates for linezolid CL. However, they were unable to identify that RF influenced linezolid CL; this may have been because of their empirical approach, with only 52 critically ill patients. Other reports have clearly identified that impaired RF is associated with lower linezolid CL [20, 24, 34, 37].

We used a size-independent measure of RF to account for renal impairment and estimate both renal and nonrenal components of CL. This clearly demonstrated an important role for the renal elimination of linezolid. After accounting for the effects of size, RF and plasma protein binding, we found a small decrease in nonrenal CL with increasing age (2% per year).

A comparison of our estimates of pharmacokinetic parameters with those reported in the literature is shown in Table 3. CL was somewhat lower than reported by others, although it is difficult to compare estimates when the original values were not reported in a standardized fashion. This was particularly challenging when RF was not included in the reported model. Studies including healthy subjects might be expected to have higher CL but there was no evidence for this.

The pcVPC of unbound concentrations of linezolid (Figure 3) showed that the predictions matched the observed concentrations initially but that the observed values were underpredicted from day 3 to day 14. This would be consistent with the proposal by Plock *et al.* [52] that linezolid inhibits its own metabolism, although the magnitude of the effect observed the present study was much smaller (10%) than that predicted (75%). Implementation of this model did not improve the fit. It is unlikely that changes in plasma protein binding would cause this effect because linezolid is bound to albumen and albumen levels are reduced in sick patients [69, 70].

The estimated parameters describing platelet turnover were similar to those of previous studies [34, 37]. The results of our data analysis indicated that the population mean values of MTT, feedback parameter (γ) with an absolute value and PLTZERO were 113 h, 0.187 and 206 000 µl^{-1}, respectively. A comparison of pharmacodynamic parameters of the previous study with those in this study is shown in Table 4. The estimated platelet turnover time (MTT), feedback parameter γ and linezolid potency (SLOPE) in the current study were similar to those reported by Sasaki *et al.* [34]. Boak *et al.* [37] reported an MTT about 50% longer and a γ five times larger and a SLOPE 10 times larger.

Previous reports regarding linezolid-induced thrombocytopenia proposed two mechanisms involving the increased elimination of platelets either by non-immune-mediated thrombocytopenia caused by bone marrow suppression [34, 36, 37, 71] or by linezolid-induced platelet destruction [40, 42]. Loo *et al.* [72] suggested that both of these mechanisms of linezolid-induced thrombocytopenia may involve immune-related pathways.

The mechanism-based turnover model we have described for linezolid-induced thrombocytopenia involves either PDI or PDS. The platelet turnover models described in previous studies of linezolid have explained the decrease in the number of platelets by an inhibitory mechanism without exploring the possibility of stimulated elimination [34, 37]. Sasaki *et al.* [34] reported linezolid-induced inhibition of platelet proliferation, whereas Boak *et al.* [37] reported linezolid-induced inhibition of platelet stem cells. We tested both of these platelet inhibition models and found a better fit based on inhibition of platelet proliferation. We are not aware of a specific mechanism explaining how linezolid impairs platelet proliferation.

Based on a mixture model in the present study for the distribution of patient responses, it appears that linezolid-induced PDS occurred in only 3% of patients compared with 97% for linezolid induced PDI. It is not possible directly to distinguish whether or not the stimulation of an elimination mechanism is immune mediated [72, 73]. However, the low value for SC50 (0.33 mg l^{-1} total plasma concentration compared with observed concentrations greater than 1 mg l^{-1}) is consistent with an immune-related mechanism initiated by very low levels of exposure. Caution is required in this interpretation because of the large %RSE and wide bootstrap confidence interval (0.00004, 1.405 mg l^{-1}) for SC50.

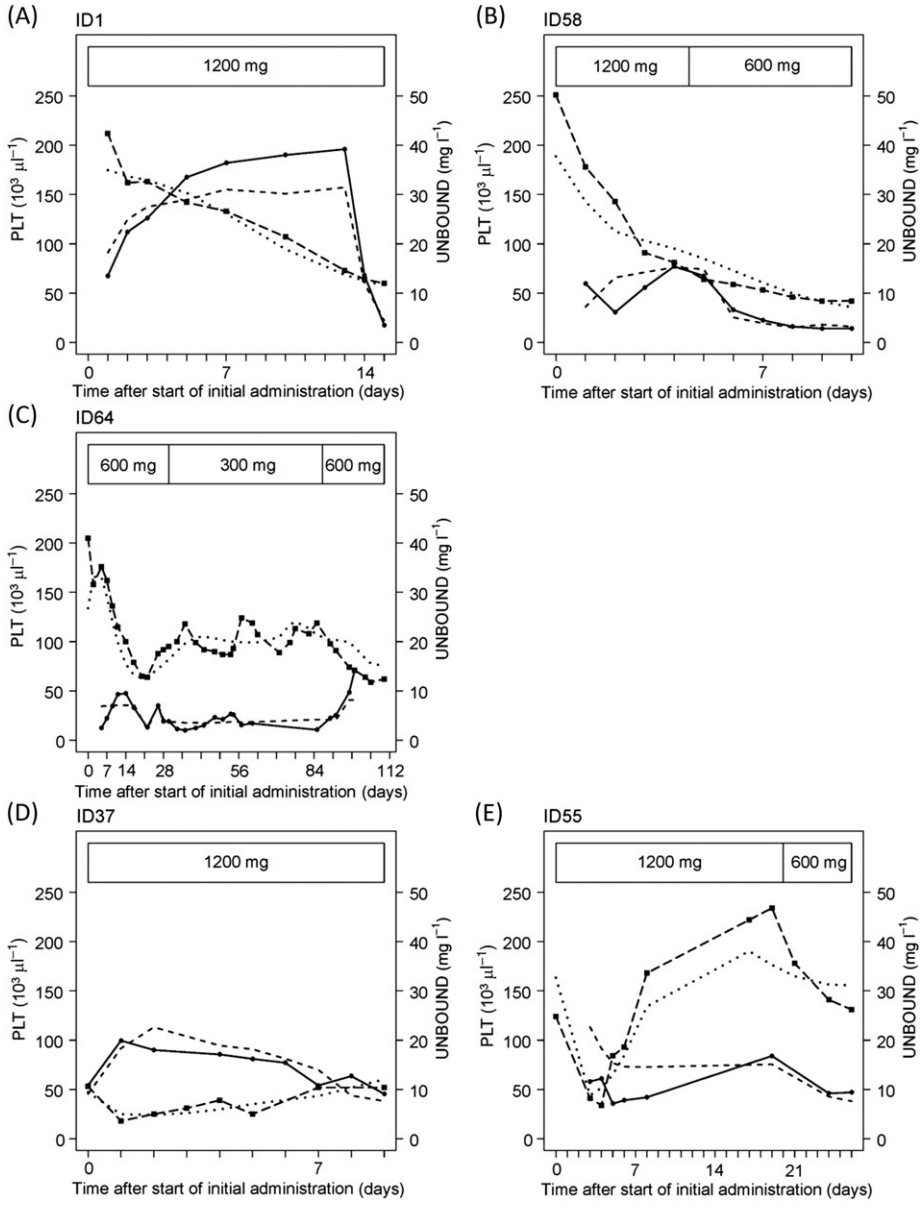

Figure 6

Time course of platelet count and unbound plasma linezolid concentration in representative patients having different dosages and durations of linezolid administration. Patients 1, 58 and 64 (A–C) are best described as showing inhibition of the synthesis of platelets. Patients 37 and 55 (D and E) are patients that are best described as showing stimulation of the elimination of platelets. Boxed areas show linezolid duration and dosage per day. closed circle and solid line, observed unbound plasma linezolid concentration; dashed line, predicted unbound plasma linezolid concentration using the final model; closed square and long-dashed line, observed platelet count; dotted line, predicted platelet count; PLT, platelet count; UNBOUND, unbound plasma linezolid concentration

Impaired RF and the use of linezolid is associated with a decrease in platelet count [19, 21, 23, 25, 26, 34]. This could be due to an effect of renal impairment on platelets as well as an increased inhibition of platelet proliferation associated with increased linezolid concentrations. Alternatively, it could simply be due to increased inhibition of platelet proliferation because of elevated linezolid concentrations. We were not able to detect any additional effect of RF on linezolid-induced inhibition. This indicates that linezolid-induced thrombocytopenia is due only to linezolid and it is not made worse by renal impairment independently of linezolid concentration.

When the mechanism appears to be inhibition of proliferation, the onset of the decrease in platelet count is delayed and reaches a nadir at around 2 weeks (Figure 5). By contrast, when the mechanism appears to be stimulation of elimination, the nadir is reached at around 2 days (Figure 5).

We used our model to predict the time course of linezolid concentrations and platelet counts before and after a period of linezolid treatment in some individual patients to

Table 3

Comparison of pharmacokinetic parameters (average, BSV%) of linezolid estimated in this study with those in the literature

	Type of subject	CL (l h^{-1} 70 kg^{-1})	VC (l 70 kg^{-1})	VP (l 70 kg^{-1})	Q (l h^{-1} 70 kg^{-1})	Ka (h^{-1})	T_{abs} (h)	F	T half (h)
Present study:	Patient	3.3 (36.9)	22.9 (142)	24.7 (5.0)	10.9 (182)	0.19	3.61	0.92	10.0
Literature studies:									
Matsumoto *et al.* [20]	Patient	4.61 (30.5)[a]	27.6 [a]						4.1
Sasaki *et al.* [34]	Patient	3.87 (35.2)	40.6 (30.8)						7.3
Boak *et al.* [37]	Patient	6.72 (48.9)	47.7 (3.6)			4.04	0.17 (14.7)		4.7
Abe *et al.* [53]	Patient	5.34 (46.6)	47.3 (25.9)			0.58 (327)	1.19		6.1
Adembri *et al.* [54]	Patient	13.0[a]	55.7						3.0
Beringer *et al.* [55]	Patient	8.82[a]	60.2			0.75	0.92	0.88	4.7
Keel *et al.* [56]	Patient	9.54 (36.3)[a]	26.8[a]	17.3 (85.8)	104	1.91	0.36	0.85 (23.0)	3.2
Meagher *et al.* [57]	Patient	7.38 (50.3)	42.7 (22.7)	28.2	9.09	5.73	0.12		6.7
Plock *et al.* [52]	Healthy and patient	2.67[b] (41.7)[a]	20.0 (40.1)	28.9 (34.8)	75.0	1.81 (72.4)	0.38		3.1
Welshman *et al.* [58]	Healthy	8.76[a]	62.6					1.03	5.0
Whitehouse *et al.* [59]	Patient	3.41 (48.1)[a]	44.4 (22.4)	240 (146)	7.48				57.8
Taubert *et al.* [60]	Patient	7.92 (58.0)[a]	13.5 (37.0)	26.6		1.72	0.40		3.5

Literature estimates of parameters were standardized based on a total body weight of 70 kg and creatinine CL of 6 l h^{-1} 70 kg^{-1} when possible. Between-subject variability (BSV%) was calculated by 100 × sqrt (NONMEM OMEGA). Ka was calculated as the natural logarithm of 2 (Ln (2)) divided by T_{abs} or T_{abs} as Ln (2)/Ka; T half was calculated as Ln (2)*(VC + VP)/CL

[a]Not standardized

[b]Calculated at 10 mg l^{-1} total concentration

CL, clearance; F, absolute bioavailability; Ka, absorption rate constant; Q, inter-compartment clearance; T half, elimination half-life; T_{abs}, absorption half-life; VC, volume of the central compartment; VP, volume of the peripheral compartment

Table 4

Comparison of pharmacodynamic parameters (average, BSV%) of linezolid estimated in the present study with two literature studies

Authors	Type of subject	MTT (h)	γ	PLTZERO (μl^{-1})	SLOPE 1/(mg l^{-1})	SMAX	SC50 (ml^{-1})
Present study:	Patient	113 (23.9)	–0.187 (30.7)	206 000 (57.0)	0.00566 (47.3)	2.55	0.00364
Literature studies:							
Sasaki *et al.* [34]	Patient	110 (33.9)	–0.203	253 000 (45.9)	0.00416 (93.8)		
Boak *et al.* [37]	Patient	163 (20.3)	–1.02	252 000 (65.1)	0.055 (at 10 mg l^{-1})		

Between-subject variability (BSV%) was calculated from 100 × Square root (NONMEM OMEGA)γ, feedback parameter; MTT, mean transit time; PLTZERO, baseline platelet count; SLOPE, slope of inhibition effect; SMAX, maximal extent of stimulation effect; SC50, linezolid total plasma concentration producing 50% of the maximum stimulation effect

illustrate the typical behaviour according to the two mechanisms we describe for thrombocytopenia (Figure 6). We also show the predictions for one patient who was originally identified to be in the PDS group erroneously because they already had thrombocytopenia before starting treatment with linezolid. We removed this patient from the final analysis dataset.

These results were in good agreement with the timing of the platelet count nadir previously described as non-

immune-mediated thrombocytopenia (PDI) [34, 36, 37, 71, 72] and immune-mediated thrombocytopenia (PDS) [40, 42, 72]. In view of these results, we recommend that platelet count monitoring should be considered for all patients immediately before the start of linezolid treatment, and then on days 2 and 4 and weeks 1, 2 and 3.

A Bayesian dosing method has been developed using the linezolid model described here. It is part of the web-based NextDose tool, which is designated for use in a clinical environment. Instructions for access to NextDose are available at www.nextdose.org.

Several limitations of the present study warrant mention. First, bone marrow samples were not available. These would have allowed the differentiation process from haematopoietic cells to megakaryocytes or megakaryocytic differentiation to be studied. It would then have been possible to have a clearer understanding of the mechanism of linezolid-induced thrombocytopenia. Second, we could not be sure whether other diseases and/or other drugs have an effect on platelet count. Third, we had very few patients with rapid loss of platelets. However, two patients (ID 37 and 55) appeared to demonstrate this mechanism, as shown by Figure 6. Finally, because the heights of patients were not recorded, we could not predict normal fat mass [74] and therefore gain an understanding of how body composition influences the size relationship for linezolid pharmacokinetic parameters.

We have described the influence of weight, RF, age and plasma protein binding on the pharmacokinetics of linezolid. This pharmacokinetic model allowed us to determine that the most common mechanism for thrombocytopenia associated with linezolid is PDI. Increased exposure with renal impairment is predictable and thrombocytopenia avoidable by dose reduction. Target concentration intervention to optimize linezolid exposure is expected to reduce the risk of thrombocytopenia.

Competing Interests

All authors have completed the Unified Competing Interest form at http://www.icmje.org/coi_disclosure.pdf (available on request from the corresponding author) and declare no support from any organization for the submitted work, no financial relationships with any organizations that might have an interest in the submitted work in the previous 3 years; no other relationships or activities that could appear to have influenced the submitted work.

Contributors

Y.T. contributed to the acquisition of data, analysed and interpreted data, participated in study design and drafted the manuscript. N.H.G.H. analysed and interpreted data and revised the manuscript. H.K., Y.A.H. and H.T. contributed to the study conception and design, and interpretation of the data. C.O. contributed to plasma concentration measurements. Y.H., A.M. and Y.Y. were the clinical investigators of the trial and responsible for the medical care of trial participants, communication with the research ethics committee, protocol, informed consent, data integrity and reporting. All authors approved the final version to be published.

References

1 Zurenko GE, Yagi BH, Schaadt RD, Allison JW, Kilburn JO, Glickman SE, *et al*. *In vitro* activities of U-100592 and U-100766, novel oxazolidinone antibacterial agents. Antimicrob Agents Chemother 1996; 40: 839–45.

2 Dryden MS. Linezolid pharmacokinetics and pharmacodynamics in clinical treatment. J Antimicrob Chemother 2011; 66 (Suppl. 4)): iv7–iv15.

3 Lovering AM, Zhang J, Bannister GC, Lankester BJA, Brown JHM, Narendra G, *et al*. Penetration of linezolid into bone, fat, muscle and haematoma of patients undergoing routine hip replacement. J Antimicrob Chemother 2002; 50: 73–7.

4 Tsuji Y, Hashimoto W, Taniguchi S, Hiraki Y, Mizoguchi A, Yukawa E, *et al*. Pharmacokinetics of linezolid in the mediastinum and pleural space. Int J Infect Dis 2013; 17: E1060–E1061.

5 Tsuji Y, Hiraki Y, Matsumoto K, Mizoguchi A, Sadoh S, Kobayashi T, *et al*. Pharmacokinetics and protein binding of linezolid in cerebrospinal fluid and serum in a case of post-neurosurgical bacterial meningitis. Scand J Infect Dis 2011; 43: 982–5.

6 Tsuji Y, Tashiro M, Ashizawa N, Ota Y, Obi H, Nagura S, *et al*. Treatment of mediastinitis due to methicillin-resistant *Staphylococcus aureus* in a renal dysfunction patient undergoing adjustments to the linezolid dose. Intern Med 2015; 54: 235–9.

7 Noskin GA, Siddiqui F, Stosor V, Hacek D, Peterson LR. *In vitro* activities of linezolid against important Gram-positive bacterial pathogens including vancomycin-resistant enterococci. Antimicrob Agents Chemother 1999; 43: 2059–62.

8 Shinabarger D. Mechanism of action of the oxazolidinone antibacterial agents. Expert Opin Investig Drugs 1999; 8: 1195–202.

9 Cosgrove SE, Qi Y, Kaye KS, Harbarth S, Karchmer AW, Carmeli Y. The impact of methicillin resistance in *Staphylococcus aureus* bacteremia on patient outcomes: mortality, length of stay, and hospital charges. Infect Control Hosp Epidemiol 2005; 26: 166–74.

10 Shorr AF, Combes A, Kollef MH, Chastre J. Methicillin-resistant *Staphylococcus aureus* prolongs intensive care unit stay in ventilator-associated pneumonia, despite initially appropriate antibiotic therapy. Crit Care Med 2006; 34: 700–6.

11 Wunderink RG, Niederman MS, Kollef MH, Shorr AF, Kunkel MJ, Baruch A, *et al*. Linezolid in methicillin-resistant *Staphylococcus aureus* nosocomial pneumonia: a randomized, controlled study. Clin Infect Dis 2012; 54: 621–9.

12 Rubinstein E, Cammarata S, Oliphant T, Wunderink R, Linezolid Nosocomial Pneumonia Study Group. Linezolid (PNU-100766) versus vancomycin in the treatment of hospitalized patients with nosocomial pneumonia: a randomized, double-blind, multicenter study. Clin Infect Dis 2001; 32: 402–12.

13 Wunderink RG, Cammarata SK, Oliphant TH, Kollef MH, Linezolid Nosocomial Pneumonia Study Group. Continuation of a randomized, double-blind, multicenter study of linezolid versus

vancomycin in the treatment of patients with nosocomial pneumonia. Clin Ther 2003; 25: 980–92.

14 Kollef MH, Rello J, Cammarata SK, Croos-Dabrera RV, Wunderink RG. Clinical cure and survival in Gram-positive ventilator-associated pneumonia: retrospective analysis of two double-blind studies comparing linezolid with vancomycin. Intensive Care Med 2004; 30: 388–94.

15 Kalil AC, Klompas M, Haynatzki G, Rupp ME. Treatment of hospital-acquired pneumonia with linezolid or vancomycin: a systematic review and meta-analysis. BMJ Open 2013; 3: e003912.

16 Walkey AJ, O'Donnell MR, Wiener RS. Linezolid *vs*. glycopeptide antibiotics for the treatment of suspected methicillin-resistant *Staphylococcus aureus* nosocomial pneumonia: a meta-analysis of randomized controlled trials. Chest 2011; 139: 1148–55.

17 Wang Y, Zou Y, Xie J, Wang T, Zheng X, He H, *et al*. Linezolid versus vancomycin for the treatment of suspected methicillin-resistant *Staphylococcus aureus* nosocomial pneumonia: a systematic review employing meta-analysis. Eur J Clin Pharmacol 2015; 71: 107–15.

18 Brier ME, Stalker DJ, Aronoff GR, Batts DH, Ryan KK, O'Grady M, *et al*. Pharmacokinetics of linezolid in subjects with renal dysfunction. Antimicrob Agents Chemother 2003; 47: 2775–80.

19 Cossu AP, Musu M, Mura P, De Giudici LM, Finco G. Linezolid-induced thrombocytopenia in impaired renal function: is it time for a dose adjustment? A case report and review of literature. Eur J Clin Pharmacol 2014; 70: 23–8.

20 Matsumoto K, Shigemi A, Takeshita A, Watanabe E, Yokoyama Y, Ikawa K, *et al*. Analysis of thrombocytopenic effects and population pharmacokinetics of linezolid: a dosage strategy according to the trough concentration target and renal function in adult patients. Int J Antimicrob Agents 2014; 44: 242–7.

21 Matsumoto K, Takeda Y, Takeshita A, Fukunaga N, Shigemi A, Yaji K, *et al*. Renal function as a predictor of linezolid-induced thrombocytopenia. Int J Antimicrob Agents 2009; 33: 98–9.

22 Pea F, Viale P, Cojutti P, Del Pin B, Zamparini E, Furlanut M. Therapeutic drug monitoring may improve safety outcomes of long-term treatment with linezolid in adult patients. J Antimicrob Chemother 2012; 67: 2034–42.

23 Tsuji Y, Hiraki Y, Matsumoto K, Mizoguchi A, Kobayashi T, Sadoh S, *et al*. Thrombocytopenia and anemia caused by a persistent high linezolid concentration in patients with renal dysfunction. J Infect Chemother 2011; 17: 70–5.

24 Tsuji Y, Yukawa E, Hiraki Y, Matsumoto K, Mizoguchi A, Morita K, *et al*., To H. Population pharmacokinetic analysis of linezolid in low body weight patients with renal dysfunction. J Clin Pharmacol 2013; 53: 967–73.

25 Wu VC, Wang YT, Wang CY, Tsai IJ, Wu KD, Hwang JJ, *et al*. High frequency of linezolid-associated thrombocytopenia and anemia among patients with end-stage renal disease. Clin Infect Dis 2006; 42: 66–72.

26 Nukui Y, Hatakeyama S, Okamoto K, Yamamoto T, Hisaka A, Suzuki H, *et al*. High plasma linezolid concentration and impaired renal function affect development of linezolid-induced thrombocytopenia. J Antimicrob Chemother 2013; 68: 2128–33.

27 Pea F, Cojutti P, Dose L, Baraldo M. A one-year retrospective audit of quality indicators of clinical pharmacological advice for personalized linezolid dosing: one stone for two birds? Br J Clin Pharmacol 2015; 81: 341–8.

28 Birmingham MC, Rayner CR, Meagher AK, Flavin SM, Batts DH, Schentag JJ. Linezolid for the treatment of multidrug-resistant, Gram-positive infections: experience from a compassionate-use program. Clin Infect Dis 2003; 36: 159–68.

29 Sotgiu G, Centis R, D'Ambrosio L, Alffenaar JW, Anger HA, Caminero JA, *et al*. Efficacy, safety and tolerability of linezolid containing regimens in treating MDR-TB and XDR-TB: systematic review and meta-analysis. Eur Respir J 2012; 40: 1430–42.

30 Gerson SL, Kaplan SL, Bruss JB, Le V, Arellano FM, Hafkin B, *et al*. Hematologic effects of linezolid: summary of clinical experience. Antimicrob Agents Chemother 2002; 46: 2723–6.

31 Niwa T, Suzuki A, Sakakibara S, Kasahara S, Yasuda M, Fukao A, *et al*. Retrospective cohort chart review study of factors associated with the development of thrombocytopenia in adult Japanese patients who received intravenous linezolid therapy. Clin Ther 2009; 31: 2126–33.

32 Attassi K, Hershberger E, Alam R, Zervos MJ. Thrombocytopenia associated with linezolid therapy. Clin Infect Dis 2002; 34: 695–8.

33 Takahashi Y, Takesue Y, Nakajima K, Ichiki K, Tsuchida T, Tatsumi S, *et al*. Risk factors associated with the development of thrombocytopenia in patients who received linezolid therapy. J Infect Chemother 2011; 17: 382–7.

34 Sasaki T, Takane H, Ogawa K, Isagawa S, Hirota T, Higuchi S, *et al*. Population pharmacokinetic and pharmacodynamic analysis of linezolid and a hematologic side effect, thrombocytopenia, in Japanese patients. Antimicrob Agents Chemother 2011; 55: 1867–73.

35 Hiraki Y, Tsuji Y, Hiraike M, Misumi N, Matsumoto K, Morita K, *et al*. Correlation between serum linezolid concentration and the development of thrombocytopenia. Scand J Infect Dis 2012; 44: 60–4.

36 Green SL, Maddox JC, Huttenbach ED. Linezolid and reversible myelosuppression. JAMA 2001; 285: 1291.

37 Boak LM, Rayner CR, Grayson ML, Paterson DL, Spelman D, Khumra S, *et al*. Clinical population pharmacokinetics and toxicodynamics of linezolid. Antimicrob Agents Chemother 2014; 58: 2334–43.

38 Friberg LE, Henningsson A, Maas H, Nguyen L, Karlsson MO. Model of chemotherapy-induced myelosuppression with parameter consistency across drugs. J Clin Oncol 2002; 20: 4713–21.

39 Harker LA, Marzec UM, Hunt P, Kelly AB, Tomer A, Cheung E, *et al*. Dose–response effects of pegylated human megakaryocyte growth and development factor on platelet production and function in nonhuman primates. Blood 1996; 88: 511–21.

40 Bernstein WB, Trotta RF, Rector JT, Tjaden JA, Barile AJ. Mechanisms for linezolid-induced anemia and thrombocytopenia. Ann Pharmacother 2003; 37: 517–20.

41 De Vriese AS, Coster RV, Smet J, Seneca S, Lovering A, Van Haute LL, *et al*. Linezolid-induced inhibition of mitochondrial protein synthesis. Clin Infect Dis 2006; 42: 1111–7.

42 Pascoalinho D, Vilas MJ, Coelho L, Moreira P. Linezolid-related immune-mediated severe thrombocytopenia. Int J Antimicrob Agents 2011; 37: 88–9.

43 Zhang L, Beal SL, Sheiner LB. Simultaneous *vs*. sequential analysis for population PK/PD data I: best-case performance. J Pharmacokinet Pharmacodyn 2003; 30: 387–404.

44 Zhang L, Beal SL, Sheinerz LB. Simultaneous *vs*. sequential analysis for population PK/PD data II: robustness of methods. J Pharmacokinet Pharmacodyn 2003; 30: 405–16.

45 Holford N, Heo YA, Anderson B. A pharmacokinetic standard for babies and adults. J Pharm Sci 2013; 102: 2941–52.

46 Anderson BJ, Holford NHG. Mechanistic basis of using body size and maturation to predict clearance in humans. Drug Metab Pharmacokinet 2009; 24: 25–36.

47 Cockcroft DW, Gault MH. Prediction of creatinine clearance from serum creatinine. Nephron 1976; 16: 31–41.

48 Matthews I, Kirkpatrick C, Holford N. Quantitative justification for target concentration intervention – parameter variability and predictive performance using population pharmacokinetic models for aminoglycosides. Br J Clin Pharmacol 2004; 58: 8–19.

49 Mould DR, Holford NH, Schellens JH, Beijnen JH, Hutson PR, Rosing H, *et al*. Population pharmacokinetic and adverse event analysis of topotecan in patients with solid tumors. Clin Pharmacol Ther 2002; 71: 334–48.

50 Parke J, Holford NH, Charles BG. A procedure for generating bootstrap samples for the validation of nonlinear mixed-effects population models. Comput Methods Programs Biomed 1999; 59: 19–29.

51 Bergstrand M, Hooker AC, Wallin JE, Karlsson MO. Prediction-corrected visual predictive checks for diagnosing nonlinear mixed-effects models. AAPS J 2011; 13: 143–51.

52 Plock N, Buerger C, Joukhadar C, Kljucar S, Kloft C. Does linezolid inhibit its own metabolism? Population pharmacokinetics as a tool to explain the observed nonlinearity in both healthy volunteers and septic patients. Drug Metab Dispos 2007; 35: 1816–23.

53 Abe S, Chiba K, Cirincione B, Grasela TH, Ito K, Suwa T. Population pharmacokinetic analysis of linezolid in patients with infectious disease: application to lower body weight and elderly patients. J Clin Pharmacol 2009; 49: 1071–8.

54 Adembri C, Fallani S, Cassetta MI, Arrigucci S, Ottaviano A, Pecile P, *et al*. Linezolid pharmacokinetic/pharmacodynamic profile in critically ill septic patients: intermittent versus continuous infusion. Int J Antimicrob Agents 2008; 31: 122–9.

55 Beringer P, Nguyen M, Hoem N, Louie S, Gill M, Gurevitch M, *et al*. Absolute bioavailability and pharmacokinetics of linezolid in hospitalized patients given enteral feedings. Antimicrob Agents Chemother 2005; 49: 3676–81.

56 Keel RA, Schaeftlein A, Kloft C, Pope JS, Knauft RF, Muhlebach M, *et al*. Pharmacokinetics of intravenous and oral linezolid in adults with cystic fibrosis. Antimicrob Agents Chemother 2011; 55: 3393–8.

57 Meagher AK, Forrest A, Rayner CR, Birmingham MC, Schentag JJ. Population pharmacokinetics of linezolid in patients treated in a compassionate-use program. Antimicrob Agents Chemother 2003; 47: 548–53.

58 Welshman IR, Sisson TA, Jungbluth GL, Stalker DJ, Hopkins NK. Linezolid absolute bioavailability and the effect of food on oral bioavailability. Biopharm Drug Dispos 2001; 22: 91–7.

59 Whitehouse T, Cepeda JA, Shulman R, Aarons L, Nalda-Molina R, Tobin C, *et al*. Pharmacokinetic studies of linezolid and teicoplanin in the critically ill. J Antimicrob Chemother 2005; 55: 333–40.

60 Taubert M, Zoller M, Maier B, Frechen S, Scharf C, Holdt LM, *et al*. Predictors of inadequate linezolid concentrations after standard dosing in critically ill patients. Antimicrob Agents Chemother 2016; 60: 5254–61.

61 Bailey EM, Rybak MJ, Kaatz GW. Comparative effect of protein binding on the killing activities of teicoplanin and vancomycin. Antimicrob Agents Chemother 1991; 35: 1089–92.

62 Nix DE, Matthias KR, Ferguson EC. Effect of ertapenem protein binding on killing of bacteria. Antimicrob Agents Chemother 2004; 48: 3419–24.

63 Schmidt S, Rock K, Sahre M, Burkhardt O, Brunner M, Lobmeyer MT, *et al*. Effect of protein binding on the pharmacological activity of highly bound antibiotics. Antimicrob Agents Chemother 2008; 52: 3994–4000.

64 Wise R. The clinical relevance of protein binding and tissue concentrations in antimicrobial therapy. Clin Pharmacokinet 1986; 11: 470–82.

65 Zeitlinger MA, Sauermann R, Traunmuller F, Georgopoulos A, Muller M, Joukhadar C. Impact of plasma protein binding on antimicrobial activity using time-killing curves. J Antimicrob Chemother 2004; 54: 876–80.

66 Buerger C, Plock N, Dehghanyar P, Joukhadar C, Kloft C. Pharmacokinetics of unbound linezolid in plasma and tissue interstitium of critically ill patients after multiple dosing using microdialysis. Antimicrob Agents Chemother 2006; 50: 2455–63.

67 Traunmuller F, Schintler MV, Spendel S, Popovic M, Mauric O, Scharnagl E, *et al*. Linezolid concentrations in infected soft tissue and bone following repetitive doses in diabetic patients with bacterial foot infections. Int J Antimicrob Agents 2010; 36: 84–6.

68 Yagi T, Naito T, Doi M, Nagura O, Yamada T, Maekawa M, *et al*. Plasma exposure of free linezolid and its ratio to minimum inhibitory concentration varies in critically ill patients. Int J Antimicrob Agents 2013; 42: 329–34.

69 Don BR, Kaysen G. Serum albumin: relationship to inflammation and nutrition. Semin Dial 2004; 17: 432–7.

70 Sleep D. Albumin and its application in drug delivery. Expert Opin Drug Deliv 2015; 12: 793–812.

71 Ebeling F, Helminen P, Anttila VJ. Appearance of ring sideroblasts in bone marrow during linezolid therapy. Scand J Infect Dis 2009; 41: 480–2.

72 Loo AS, Gerzenshtein L, Ison MG. Antimicrobial drug-induced thrombocytopenia: a review of the literature. Semin Thromb Hemost 2012; 38: 818–29.

73 Aster RH, Bougie DW. Drug-induced immune thrombocytopenia. N Engl J Med 2007; 357: 580–7.

74 Anderson BJ, Holford NHG. Mechanistic basis of using body size and maturation to predict clearance in humans. Drug Metab Pharmacokinet 2009; 24: 25–36.